Research Article

Inertial Forces and Torques Acting on a Spinning Annulus

Ryspek Usubamatov [1] **and Sarken Kapayeva** [2]

[1]*Kyrgyz State Technical University after I. Razzakov, Bishkek, Kyrgyzstan*
[2]*East Kazakhstan Technical University after D. Serikbaev, Kazakhstan*

Correspondence should be addressed to Ryspek Usubamatov; ryspek0701@yahoo.com

The many publications related to the gyroscope theory consider the action of the inertial torques on the spinning disc. All of them have simplified expressions for the inertial torques and mathematical models of the gyroscope motions do not validate by practice. Recent research in the theory of the gyroscopic effects for rotating objects solved problems with mathematical models for interrelated inertial torques generated by the spinning disc, bar, and ring and their motions. Practitioners of engineering designed gyroscopic devices with spinning rotors whose geometry can be an annulus or similar designs. Such spinning annulus generates inertial torques whose expressions differ from the disc bar and ring and hence another mathematical model describes the motions of the gyroscopic devices. The value of gyroscopic effects of the devices with spinning annulus is bigger than for the disc-type rotor. This manuscript presents mathematical models for the inertial torques generated by the spinning annulus and the interrelated angular velocities of the gyroscopic devices about axes of rotation.

1. Introduction

The gyroscopic effects in engineering mechanics are the most complex problems that are being unsolved for a long time [1–5]. Beginning from the Industrial Revolution, scientists yield only partial analytical solutions but did not solve the entire gyroscopic effects. For practical applications were worked out numerical models with the expensive software for gyroscopic effects. The physics of the gyroscopic effects of the simple spinning disc remained unexplained and mysterious for a couple of centuries [6–10]. Scientists and researchers of our time continue to describe gyroscopic effects without success which can be seen in many publications each year [11–19]. Recent investigations of the gyroscopic effects showed their nature is more complex and based on several physical principles that were discovered at different times. Scientists of 18-19 centuries could not solve gyroscopic effects in principle because the concept of mechanical energy conservation was formulated at the beginning of twenty century. From this time, researchers have all the analytical tools for formulation of the gyroscope theory but did not do it.

The latest studies of the physics of the gyroscopic effects yield mathematical models for the inertial torques and the interrelated dependency of the angular velocities of the spinning disc motions about axes of rotation. The solution to gyroscopic effects is based on the principle of mechanical energy conservation [20–22]. The method of deriving mathematical models for inertial torques shows the action of the system of the centrifugal, Coriolis forces generated by the rotating mass, and the change in the angular momentum of the spinning disc. The dependency of the angular velocities of the spinning disc around axes of motions interrelates the inertial torques. Table 1 presents the expressions of inertial torques acting on the spinning disc and the dependency of the angular velocities of it's motions.

The practice tests validate the action of the system of the interrelated inertial torques on the spinning disc. Practitioners should use the derived method for the modeling of the gyroscopic effects for any designs of the spinning objects [22]. The mathematical models for the inertial torques generated by the centrifugal and Coriolis forces and the change in the angular momentum acting on the spinning flat annulus and

TABLE 1: Equations of the inertial torques acting on the spinning disc.

Type of the torque generated by	Acton	Equation
Centrifugal forces	Resistance	$T_{ct} = (4/9)\pi^2 J\omega\omega_x$
	Precession	
Coriolis forces	Resistance	$T_{cr} = (8/9)J\omega\omega_x$
Change in angular momentum	Precession	$T_{am} = J\omega\omega_x$
Dependency of angular velocities of spinning disc rotations about axes		$\omega_y = (8\pi^2 + 17)\omega_x$

its interrelated motions around two axes are present as the contribution of the manuscript.

2. Centrifugal Forces and Torques Acting on a Spinning Annulus

The method for the analytical solution for all inertial torques acting on the spinning disc is described in several publications [21, 22]. The inertial torques are generated by the distributed mass elements of the spanning disc disposed on the circle of 2/3 of its radius. This method can be applied to rotating objects of different forms. For the annulus, the radius of the disposition of the distributed mass elements on the circle should be defined. The rotating mass elements produce the plane of centrifugal forces of the spinning annulus around axis oz with an angular velocity of ω in a counter-clockwise direction considered in Figure 1. The mass element m is disposed on the circle of radius r which is perpendicular to the axis of the spinning annulus.

The radius r of disposing of the mass elements of the annulus is defined from the truncated sector with the small angle $\Delta\delta$ and the arcs of the external and internal radii R_e and R_i, respectively. The rotating mass elements generate centrifugal forces. The action of the external torque to the spinning annulus has manifested the inclination of its plane with the rotating centrifugal forces and the turns of the annulus around axes. These motions are presented at the Cartesian 3D coordinate system $\Sigma oxyz$ in Figure 1. The external torque applied to the spinning annulus generates several inertial torques (Figure 2).

The plane of the rotating centrifugal forces turns around axis ox along the diameter line and changes in the directions of centrifugal force vectors f_{ct} of the mass elements. The inclined plane of rotating centrifugal forces on angle $\Delta\gamma$ around axis ox is presented in the plane $xoy *$. The action of the centrifugal force vectors f_{ct} is radial and their components $f *_{ct}$ produce the torques around axes ox and oy. The values of torques acting around axis ox are maximal at 90° and 270° and zero at 0° and 180° (Figure 2(a)). The values of torques acting around axis oy are maximal at 0° and 180° and zero at 90° and 270° (Figure 2(b)). The integrated product of the components' vector of the centrifugal forces $f_{ct.z}$ and their radii relative to axes ox and oy give the torques T_{ct} acting around two axes. The torque acting around axis ox resists the action of the external torque T. The torque acting around axis oy turns the spinning annulus in the counter-clockwise direction.

The mathematical models for the inertial torques generated by the centrifugal forces of the mass elements are expressed as follows:

$$\Delta T_{ct} = -f_{ct.z}y_m = -ma_z y_m, \tag{1}$$

$$\Delta T_{ct} = f_{ct.z}x_m = ma_z x_m, \tag{2}$$

where ΔT_{ct} is the centrifugal torque generated by the mass element; $f_{ct.z}$ is the component of the centrifugal force; y_m and x_m are the distance from the mass element to axes oy and ox, respectively; m is the mass element of the annulus disposed on the circle of the radius r; $a_z = r\omega^2$ is the radial acceleration; ω is the angular velocity of the spinning annulus; the signs (+) and (-) mean the counter-clockwise and clockwise direction, respectively.

The following equations express the component of the centrifugal force acting along axis oz:

(i) Around axis ox

$$f_{ct.z} = f_{ct} \sin\alpha \sin\Delta\gamma = mr\omega^2 \sin\alpha \sin\Delta\gamma$$
$$= \frac{Mr\omega^2}{2\pi}\Delta\delta\Delta\gamma \sin\alpha. \tag{3}$$

(ii) Around axis oy

$$f_{ct.z} = f_{ct} \cos\alpha \sin\Delta\gamma = mr\omega^2 \cos\alpha \sin\Delta\gamma$$
$$= \frac{Mr\omega^2}{2\pi}\Delta\delta\Delta\gamma \cos\alpha, \tag{4}$$

where $f_{ct} = mr\omega^2 = (Mr\omega^2/2\pi)\Delta\delta$ is the centrifugal force of the mass element m; $m = (M/2\pi r)\Delta\delta r = (M/2\pi)\Delta\delta$ in which M is the mass of the annulus; $\Delta\delta$ is the sector's angle of the mass element's disposition; α is the angle of the mass element's disposition; $\Delta\gamma$ is the angle of turn for the annulus plane, $sin\Delta\gamma = \Delta\gamma$ is the trigonometric identity for the small values of the angle.

The radius r of the circle of disposing of the mass elements m of the annulus is defined from the truncated sector with the small angle $\Delta\delta$ and the arcs of the external and internal radii R_e and R_i, respectively (Figure 1). The radius r is expressed
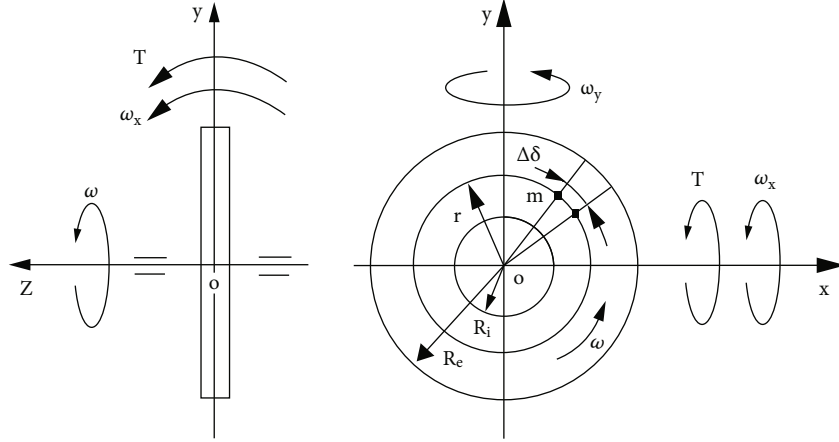
FIGURE 1: Schematic of the spinning annulus.

by the equation of the centroid of the truncated sector

$$r = \frac{\Sigma A_i r}{A_{ts}} = \frac{\left(\left(\pi R_e^2 \times (2/3) R_e \times \Delta\delta\right)/2\pi\right) - \left(\left(\pi R_i^2 \times (2/3) R_i \times \Delta\delta\right)/2\pi\right)}{\left(\pi\left(R_e^2 - R_i^2\right) \times \Delta\delta\right)/2\pi}$$
$$= \frac{2\left(R_e^3 - R_i^3\right)}{3\left(R_e^2 - R_i^2\right)},$$

(5)

where $A_e = (\pi R_e^2 \times \ \times \Delta\delta)/2\pi$ and $A_i = (\pi R_i^2 \times \ \times \Delta\delta)/2\pi$ are the area of the sectors of radii R_e and R_i and $(2/3)R_e$ and $(2/3)R_i$ are the radii of the mass elements disposition, respectively; $A_{ts} = (\pi(R_e^2 - R_i^2) \times \Delta\delta)/2\pi$ is the area of the truncated sector.

Substituting the expressions of $f_{ct.z}$ of Equations (3)–(5) into Equations (1) and (2) and transformation yield the expressions of the inertial centrifugal torques produced by the mass element.

$$\Delta T_{ct} = \frac{M\left(R_e^3 - R_i^3\right)\omega^2}{3\pi\left(R_e^2 - R_i^2\right)} \times \Delta\delta \times \Delta\gamma \times \sin\alpha \times y_m, \qquad (6)$$

$$\Delta T_{ct} = \frac{M\left(R_e^3 - R_i^3\right)\omega^2}{3\pi\left(R_e^2 - R_i^2\right)} \times \Delta\delta \times \Delta\gamma \times \cos\alpha \times x_m, \qquad (7)$$

where $y_m = r\sin\alpha$ and $x_m = r\cos\alpha$ are the distance from the mass element of the annulus relative to axes ox (Figure 2(a)) and to axis oy (Figure 2(b)), respectively; and the other components are as specified above.

The centrifugal torques are distributed on the circle where the mass elements of the annulus are located (Figures 2(a) and 2(b)). The action of the torques is defined by a concentrated load at the centroid points at the semi-circles along axes oy and ox. The known integrated equation calculates the disposition of the centroid (point A of Figure 2(a) and point B of Figure 2(b)) [6–9].

$$l_i = \frac{\int_{\alpha=0}^{\pi} f_{ct.z} l_m d\alpha}{\int_{\alpha=0}^{\pi} f_{ct.z} d\alpha}, \qquad (8)$$

where $f_{ct.z} = (M(R_e^3 - R_i^3)\omega^2/3\pi(R_e^2 - R_i^2)) \times \Delta\delta \times \Delta\gamma \times \sin\alpha$, l_i is the centroid for the semi-circle i, and l_m is y_m or x_m.

Substituting Equations (4) and (5) and other components into Equation (8) and transformation yield the following expression.

(i) About axis ox

$$\begin{aligned} y_A &= \frac{\int_{\alpha=0}^{\pi} f_{ct.z} y_m d\alpha}{\int_{\alpha=0}^{\pi} f_{ct.z} d\alpha} = \frac{\int_{\alpha=0}^{\pi} \left(M\left(R_e^3 - R_i^3\right)\omega^2/3\pi\left(R_e^2 - R_i^2\right)\right)\Delta\delta \times \Delta\gamma \times (2/3)\left(\left(R_e^3 - R_i^3\right)/\left(R_e^2 - R_i^2\right)\right)\sin\alpha\sin\alpha d\alpha}{\int_{\alpha=0}^{\pi} \left(M\left(R_e^3 - R_i^3\right)\omega^2/3\pi\left(R_e^2 - R_i^2\right)\right)\Delta\delta \times \Delta\gamma\sin\alpha d\alpha} \\ &= \frac{\left(M\left(R_e^3 - R_i^3\right)\omega^2/3\pi\left(R_e^2 - R_i^2\right)\right)\Delta\delta\Delta\gamma\int_{\alpha=0}^{\pi} 2/3R\sin^2\alpha d\alpha}{\left(M\left(R_e^3 - R_i^3\right)\omega^2/3\pi\left(R_e^2 - R_i^2\right)\right)\Delta\delta\Delta\gamma\int_{\alpha=0}^{\pi} \sin\alpha d\alpha} \\ &= \frac{(2/(3\times2))\left(\left(R_e^3 - R_i^3\right)/\left(R_e^2 - R_i^2\right)\right)\int_0^{\pi}(1-\cos 2\alpha)d\alpha}{\int_0^{\pi} \sin\alpha d\alpha} \\ &= \frac{\left(\left(R_e^3 - R_i^3\right)/3\left(R_e^2 - R_i^2\right)\right)\int_0^{\pi}(1-\cos 2\alpha)d\alpha}{\int_0^{\pi} \sin\alpha d\alpha}. \end{aligned}$$
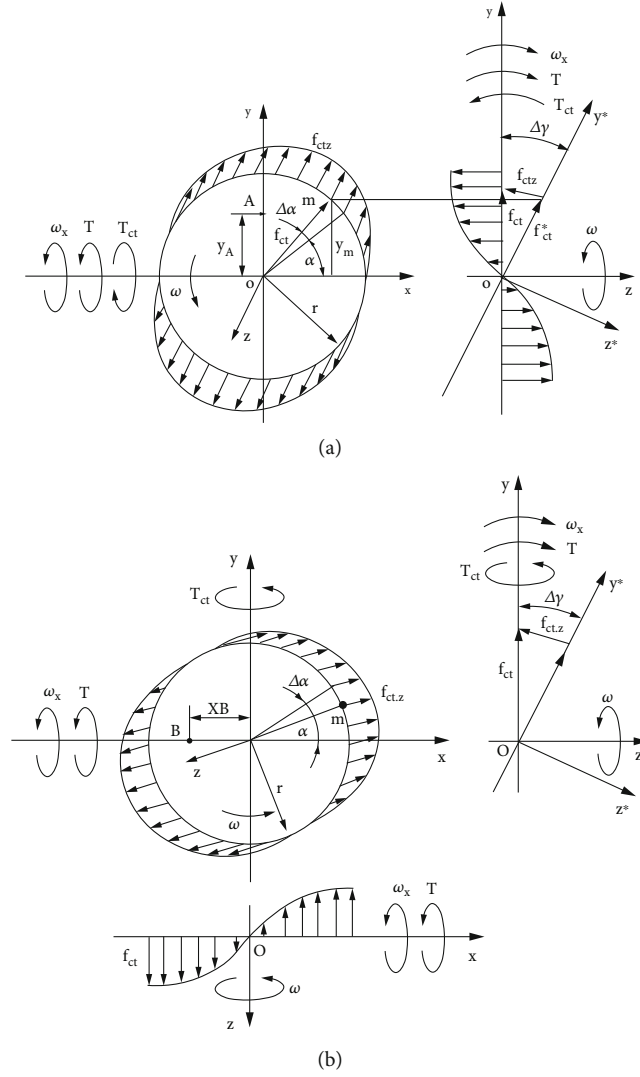
(9)

(a)

(b)

FIGURE 2: Schematic of acting centrifugal forces, torques, and motions around axis ox (a) and oy (b) of the spinning annulus.

(ii) About axis oy

$$
\begin{aligned}
x_B &= \frac{\int_{\alpha=0}^{\pi} f_{ct.z} x_m d\alpha}{\int_{\alpha=0}^{\pi} f_{ct.z} d\alpha} = \frac{\int_{\alpha=0}^{\pi} \left(M\left(R_e^3 - R_i^3\right)\omega^2/3\pi\left(R_e^2 - R_i^2\right)\right)\Delta\delta \times \Delta\gamma \times (2/3)\left(\left(R_e^3 - R_i^3\right)/\left(R_e^2 - R_i^2\right)\right)\cos\alpha\cos\alpha d\alpha}{\int_{\alpha=0}^{\pi} \left(M\left(R_e^3 - R_i^3\right)\omega^2/3\pi\left(R_e^2 - R_i^2\right)\right)\Delta\delta \times \Delta\gamma\cos\alpha d\alpha} \\
&= \frac{\left(M\left(R_e^3 - R_i^3\right)\omega^2/3\pi\left(R_e^2 - R_i^2\right)\right)\Delta\delta\Delta\gamma\int_{\alpha=0}^{\pi} 2/3R\cos^2\alpha d\alpha}{\left(M\left(R_e^3 - R_i^3\right)\omega^2/3\pi\left(R_e^2 - R_i^2\right)\right)\Delta\delta\Delta\gamma\int_{\alpha=0}^{\pi}\cos\alpha d\alpha} \\
&= \frac{(2/(3\times2))\left(\left(R_e^3 - R_i^3\right)/\left(R_e^2 - R_i^2\right)\right)\int_0^{\pi}(1+\cos2\alpha)d\alpha}{\int_0^{\pi}\cos\alpha d\alpha} \\
&= \frac{\left(\left(R_e^3 - R_i^3\right)/3\left(R_e^2 - R_i^2\right)\right)\int_0^{\pi}(1+\cos2\alpha)d\alpha}{\int_0^{\pi}\cos\alpha d\alpha},
\end{aligned}
\tag{10}
$$

where the expression $(M(R_e^3 - R_i^3)\omega^2/3\pi(R_e^2 - R_i^2))\Delta \delta \times \Delta\gamma$ is constant of Equations (9) and (10); the expressions $\sin^2\alpha = (1 - \cos 2\alpha)/2$ and $\cos^2\alpha = (1 + \cos 2\alpha)/2$ are a trigonometric identity, and other parameters are as specified above.

Equations (6) and (7) are presented in differential and integral forms. Substituting expressions of Equations (9) and (10) into Equations (6) and (7), replacing $\sin\alpha = \int_0^\pi \cos\alpha\, d\alpha$ and $\cos\alpha = -\int_0^\pi \sin\alpha\, d\alpha$ by the integral expressions with defined limits, respectively, the following equations emerge:

(i) About axis ox

$$\int_0^{T_{ct}} dT_{ct} = \frac{M(R_e^3 - R_i^3)\omega^2}{3\pi(R_e^2 - R_i^2)} \times \int_0^\pi d\delta \times \int_0^\gamma d\gamma \times \int_0^\pi \cos\alpha\, d\alpha$$
$$\times \frac{(R_e^3 - R_i^3)}{3(R_e^2 - R_i^2)} \times \frac{\int_0^\pi (1 - \cos 2\alpha) d\alpha}{\int_0^\pi \sin\alpha\, d\alpha}.$$

(11)

(ii) About axis oy

$$\int_0^{T_{ct}} dT_{ct} = \frac{M(R_e^3 - R_i^3)\omega^2}{3\pi(R_e^2 - R_i^2)} \times \int_0^\pi d\delta \times \int_0^\gamma d\gamma \times (-)\int_0^\pi \sin\alpha\, d\alpha$$
$$\times \frac{(R_e^3 - R_i^3)}{3(R_e^2 - R_i^2)} \times \frac{\int_0^\pi (1 + \cos 2\alpha) d\alpha}{\int_0^\pi \cos\alpha\, d\alpha}.$$

(12)

Solutions of integral Equations (11) and (12) yield the following:

(i) About axis ox

$$T_{ct}\Big|_0^{T_{ct}} = \frac{M}{9} \times \left(\frac{R_e^3 - R_i^3}{R_e^2 - R_i^2}\right)^2 \omega^2 \times (\delta|_0^\pi) \times (\gamma|_0^\gamma)$$
$$\times 2\left(\sin\alpha|_0^{\pi/2}\right) \times \frac{(1 - (1/2)\sin 2\alpha)|_0^\pi}{-\cos\alpha|_0^\pi}.$$

(13)

(ii) About axis oy

$$T_{ct}\Big|_0^{T_{ct}} = \frac{M}{9} \times \left(\frac{R_e^3 - R_i^3}{R_e^2 - R_i^2}\right)^2 \omega^2 \times (\delta|_0^\pi) \times (\gamma|_0^\gamma)$$
$$\times (\cos\alpha|_0^\pi) \times \frac{(1 + (1/2)\sin 2\alpha)|_0^\pi}{2\sin\alpha|_0^{\pi/2}},$$

(14)

that gave rise to the following:

(i) About axis ox

$$T_{ct} = \frac{M}{9} \left(\frac{R_e^3 - R_i^3}{R_e^2 - R_i^2}\right)^2 \omega^2 \times (\pi - 0) \times (\gamma - 0) \times 2(1 - 0)$$
$$\times \frac{[(\pi - 0) - (1/2)(0 - 0)]}{-(-1 - 1)} = \frac{M}{9}\left(\frac{R_e^3 - R_i^3}{R_e^2 - R_i^2}\right)^2 \omega^2\pi\gamma.$$

(15)

(ii) About axis oy

$$T_{ct} = \frac{M}{9}\left(\frac{R_e^3 - R_i^3}{R_e^2 - R_i^2}\right)^2 \omega^2 \times (\pi - 0) \times (\gamma - 0) \times (-1 - 1)$$
$$\times \frac{[(\pi - 0) + (1/2)(0 - 0)]}{2(1 - 0)} = -\frac{M}{9}\left(\frac{R_e^3 - R_i^3}{R_e^2 - R_i^2}\right)^2 \omega^2\pi\gamma,$$

(16)

where all components are as specified above.

Equations (15) and (16) are almost identical except for the signs ($\pm$) of counter and clockwise action around axes ox and oy. The inertial torque T_{ct} depends on the variable angle γ that expresses the angular velocity ω_x of the annulus rotation about axis ox per time t. The differential equation expresses the change in torque T_{ct} per time

$$\frac{dT_{ct}}{dt} = \pm\frac{M}{9}\left(\frac{R_e^3 - R_i^3}{R_e^2 - R_i^2}\right)^2 \omega^2\pi\frac{d\gamma}{dt},$$

(17)

where $t = \alpha/\omega$ is the time taken relative to the angular velocity of the annulus.

The differential of time t is $dt = d\alpha/\omega$; the expression $d\gamma/dt = \omega_x$ is the angular velocity of the spinning annulus around axis ox. Substituting the defined components into Equation (17) and transforming yield:

$$\frac{\omega dT_{ct}}{d\alpha} = \pm\frac{M}{9}\left(\frac{R_e^3 - R_i^3}{R_e^2 - R_i^2}\right)^2 \omega^2\omega_x\pi.$$

(18)

Separation of the variables of Equation (18), transformation, and presentation by the integral form with defined limits yield:

$$\int_0^{T_{ct}} dT_{ct} = \pm\int_0^\pi \frac{M}{9}\left(\frac{R_e^3 - R_i^3}{R_e^2 - R_i^2}\right)^2 \omega\omega_x\pi d\alpha.$$

(19)

Solution of Equation (19) yields

$$T_{ct}\Big|_0^{T_{ct}} = \pm\frac{M}{9}\left(\frac{R_e^3 - R_i^3}{R_e^2 - R_i^2}\right)^2 \omega\omega_x\pi\alpha|_0^\pi.$$

(20)

The centrifugal torques act on the upper and lower sides of the annulus about axis ox, and its left and right sides about axis oy. Then, the total torque T_{ct} acting about axes ox and oy is increased double.
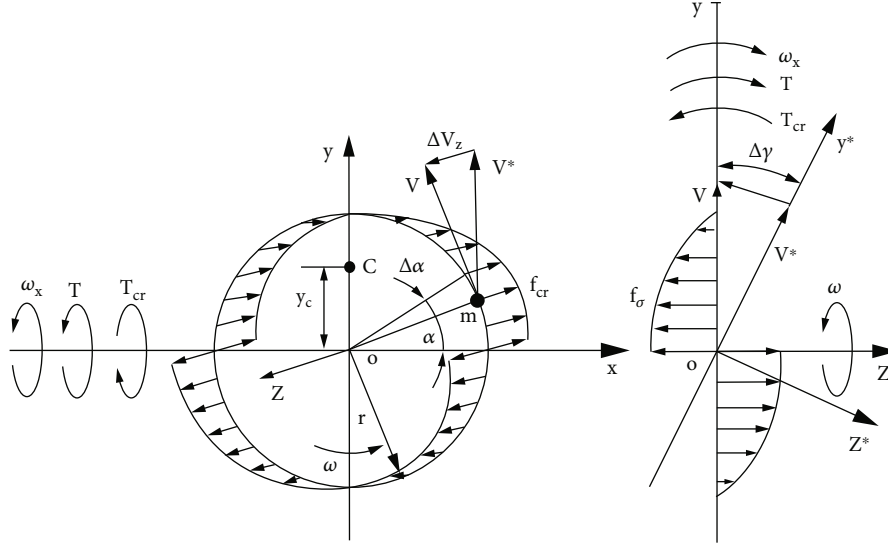
FIGURE 3: Schematic of the acting forces, torques, and motions of the spinning annulus.

$$T_{ct} = \pm \frac{2M}{9} \left(\frac{R_e^3 - R_i^3}{R_e^2 - R_i^2} \right)^2 \omega \omega_x \pi^2$$

$$= \pm \frac{4}{9 \left(R_e^2 + R_i^2 \right)} \left(\frac{R_e^3 - R_i^3}{R_e^2 - R_i^2} \right)^2 \pi^2 J \omega \omega_x, \tag{21}$$

where $J = (1/2)M(R_e^2 + R_i^2)$ is the annulus moment of inertia, and other components are as specified above.

3. Coriolis Forces and Torques Acting on a Spinning Annulus

The Coriolis acceleration and force generated by mass elements are revealed when the spinning annulus turns around axis perpendicular to its axle. The integrated Coriolis force produced by the rotating mass elements of the annulus generates the torque counteracting the external torque [10]. Figure 3 shows the rotation of the mass element m of the annulus that turns on the angle $\Delta \gamma$ around axis ox. The turn of the annulus around axis ox changes the direction of the tangential velocity vectors of mass elements. The change in the tangential velocity of mass elements produces the acceleration in which a product with a mass yields the Coriolis forces of the mass elements, where $\Delta V = V \sin \Delta \gamma$, $V = r \cos \alpha \times \omega$, and $\sin \Delta \gamma = \Delta \gamma$ for the small angle (Figure 3). The maximal changes of the velocity vectors $V*$ are on the line of axis ox. The tangential velocity V whose vector is parallel to axis ox, i.e., on 90° and 270° does not change. The changes in tangential velocity vectors are presented by the components V_z that are parallel to the annulus axle oz.

The torque generated by the Coriolis force of the rotating mass element is expressed by

$$\Delta T_{cr} = -f_{cr} y_m = -m a_z y_m, \tag{22}$$

where ΔT_{cr} is the torque generated by Coriolis force f_{cr} of the annulus mass element m; a_z is the Coriolis acceleration along with axis oz; $y_m = r \sin \alpha$ is the distance from the mass element to axis ox; the sigh (-) means the action in the clockwise direction around axis ox, and the other components are represented in Equation (2).

The differential form of changes in tangential velocity vectors is $dV/dt = a_z$ and change in the angle of rotation around axis ox is $d\gamma/dt = \omega_x$.

Then, the Coriolis acceleration is:

$$\alpha_z = r \omega_x \cos \alpha. \tag{23}$$

The Coriolis force of the mass element is presented:

$$f_{cr} = \frac{M}{2\pi} \times \Delta \delta r \omega_x \cos \alpha = \frac{M}{3\pi} \left(\frac{R_e^3 - R_i^3}{R_e^2 - R_i^2} \right) \times \Delta \delta \times \omega \omega_x \cos \alpha. \tag{24}$$

Then, the Coriolis torque is:

$$\Delta T_{cr} = -f_{cr} y_m = -\frac{M}{3\pi} \left(\frac{R_e^3 - R_i^3}{R_e^2 - R_i^2} \right) \omega \omega_x \times \Delta \delta \times \cos \alpha \times y_m, \tag{25}$$

where all parameters are as specified above.

The centroid for the torque ΔT_{cr} is point C of Figure 3, which is defined by Equation (8).

$$y_C = \frac{\int_{\alpha=0}^{\pi} f_{in.} y_m d\alpha}{\int_{\alpha=0}^{\pi} f_{in.} d\alpha} = \frac{M/3\pi \left(\left(R_e^3 - R_i^3 \right)/\left(R_e^2 - R_i^2 \right) \right) \omega \omega_x \times \Delta\delta \int_{\alpha=0}^{\pi} 2/3 \left(\left(R_e^3 - R_i^3 \right)/\left(R_e^2 - R_i^2 \right) \right) \cos\alpha \sin\alpha d\alpha}{M/3\pi \left(\left(R_e^3 - R_i^3 \right)/\left(R_e^2 - R_i^2 \right) \right) \omega \omega_x \times \Delta\delta \int_{\alpha=0}^{\pi} \sin\alpha d\alpha}$$

$$= \frac{2/3 \left(\left(R_e^3 - R_i^3 \right)/\left(R_e^2 - R_i^2 \right) \right) \int_0^{\pi} \sin\alpha d\sin\alpha}{\int_0^{\pi} \sin\alpha d\alpha}.$$

(26)

Substituting Equation (26) into Equation (25), replacing $\cos\alpha = \int_0^{\pi} - \sin\alpha d\alpha$ by the integral expression with defined limits, and presenting other components by the integral forms, the following equation emerges:

$$\int_0^{T_{cr}} dT_{cr} = -\frac{M}{3\pi} \left(\frac{R_e^3 - R_i^3}{R_e^2 - R_i^2} \right) \omega\omega_x \times \int_0^{\pi} d\delta \times \int_0^{\pi} - \sin\alpha d\alpha$$

$$\times \frac{2/3 \left(\left(R_e^3 - R_i^3 \right)/\left(R_e^2 - R_i^2 \right) \right) \int_0^{\pi} \sin\alpha d\sin\alpha}{\int_0^{\pi} \sin\alpha d\alpha}.$$

(27)

Solution of integral Equation (27) yields:

$$T_{cr}\big|_0^{cr} = -\frac{2M}{9\pi} \left(\frac{R_e^3 - R_i^3}{R_e^2 - R_i^2} \right)^2 \omega\omega_x \times \left(\delta\big|_0^{\pi} \right) \times \left(\cos\alpha\big|_0^{\pi} \right)$$

$$\times \frac{2 \left(\sin^2\alpha/2 \right)\big|_0^{\pi/2}}{2\sin\alpha\big|_0^{\pi/2}},$$

(28)

that gave rise to the following:

$$T_{cr} = -\frac{2M}{9\pi} \left(\frac{R_e^3 - R_i^3}{R_e^2 - R_i^2} \right)^2 \omega\omega_x \times (\pi - 0)$$

$$\times (-1 - 1) \times \frac{(1 - 0)}{-2(1 - 0)}$$

$$= -\frac{2M}{9} \left(\frac{R_e^3 - R_i^3}{R_e^2 - R_i^2} \right)^2 \omega\omega_x,$$

(29)

where all components are as specified above.

The inertial torque T_{cr} acts on the upper and lower sides of the annulus. Multiplying Equation (29) by two yields the full expression of T_{cr}:

$$T_{cr} = -\frac{2 \times 2M}{9} \left(\frac{R_e^3 - R_i^3}{R_e^2 - R_i^2} \right)^2 \omega\omega_x$$

$$= -\frac{8}{9\left(R_e^2 + R_i^2 \right)} \left(\frac{R_e^3 - R_i^3}{R_e^2 - R_i^2} \right)^2 J\omega_x,$$

(30)

where $J = (1/2)M(R_e^2 + R_i^2)$ is the annulus moment of inertia; the sign (-) expresses the clockwise direction.

4. Attributes of Inertial Torques Acting on a Spinning Annulus

The load torque applied to the spinning annulus produces the system of the inertial torques generated by the rotating mass [22]. Among them is the change in the angular momentum of a spinning disc, which is Euler's fundamental principle of gyroscope theory [1–5]. The motion of the spinning annulus around axis oy (Figure 3) manifests the change in the annulus angular momentum in the counter-clockwise direction which is called precession. The expression of the change in the angular momentum is $T_{am} = J\omega\omega_x$ where all components are presented above. The system of the inertial torques produces the resistance and precession torques and motions of the spinning annulus around axes of the rotation. Table 2 represents expressions of the inertial torques generated by pseudo forces of the spinning annulus.

The external torque T generates all inertial torques that depend on the mass moment of the annulus's inertia J, its angular velocity ω, and the angular velocity ω_x of the spinning annulus about axis ox.

The action of all torques around axes ox and oy on the spinning object is shown in Figure 4 for the given symmetrical disposing of its supports [22]. The interrelated action of the inertial torques is considered for the horizontal disposition of the spinning object.

The action of the inertial torques of the spinning annulus around axes ox and oy expresses analytically the equality of their mechanical energies that enables for deriving of the dependency of its interrelated angular velocities around axes of motions (Figure 4) [22].

$$-T_{ct.x} - T_{cr.x} - T_{ct.y} - T_{am.y} = T_{ct.x} + T_{am.x} - T_{ct.y} - T_{cr.y},$$

(31)

where expressions of the inertial torques are presented by Equations (21) and (30), and $T_{am} = J\omega\omega_x$.

TABLE 2: The inertial torques acting on the spinning annulus generated by the external torque.

| Type of the torque generated by	Action	Equation
Centrifugal forces, T_{ct}	Resistance Precession	$T_{ct} = \dfrac{4}{9\left(R_e^2 + R_i^2\right)}\left(\dfrac{R_e^3 - R_i^3}{R_e^2 - R_i^2}\right)^2 \pi^2 J\omega\omega_x$
Coriolis forces, T_{cr}	Resistance	$T_{cr} = \dfrac{8}{9\left(R_e^2 + R_i^2\right)}\left(\dfrac{R_e^3 - R_i^3}{R_e^2 - R_i^2}\right)^2 J\omega\omega_x$
Change in angular momentum, T_{am}	Precession	$T_{am} = J\omega\omega_x$
Dependency of angular velocities of spinning disc rotations about axes		$\omega_y = -\left[\dfrac{\left(8/\left(9\left(R_e^2 + R_i^2\right)\right)\right)\left(\left(R_e^3 - R_i^3\right)/\left(R_e^2 - R_i^2\right)\right)^2 \left(\pi^2 + 1\right) + 1}{1 - \left(8/\left(9\left(R_e^2 + R_i^2\right)\right)\right)\left(\left(R_e^3 - R_i^3\right)/\left(R_e^2 - R_i^2\right)\right)^2}\right]\omega_x$
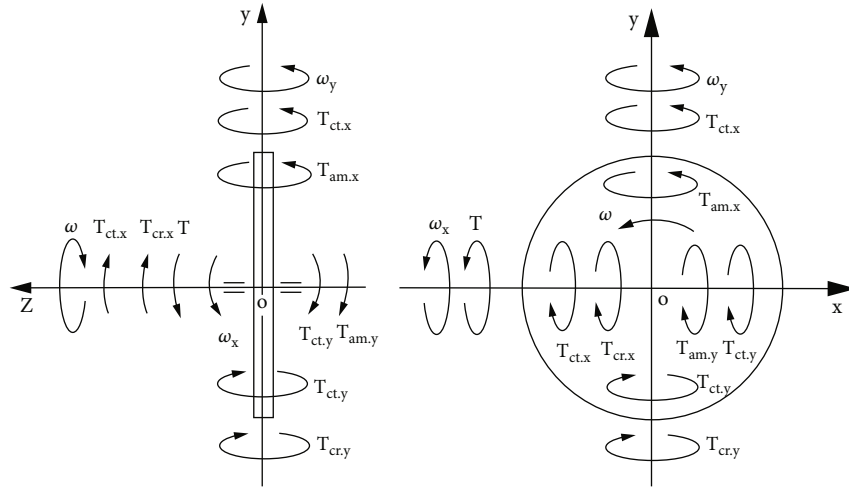
FIGURE 4: External and inertial torques acting around axes on the spinning object.

Substituting expressions of the defined torques into Equation (31) yields the following:

$$
\begin{aligned}
&-\frac{4}{9\left(R_e^2 + R_i^2\right)}\left(\frac{R_e^3 - R_i^3}{R_e^2 - R_i^2}\right)^2 \pi^2 J\omega\omega_x \\
&\quad -\frac{8}{9\left(R_e^2 + R_i^2\right)}\left(\frac{R_e^3 - R_i^3}{R_e^2 - R_i^2}\right)^2 J\omega\omega_x \\
&\quad -\frac{4}{9\left(R_e^2 + R_i^2\right)}\left(\frac{R_e^3 - R_i^3}{R_e^2 - R_i^2}\right)^2 \pi^2 J\omega\omega_y - J\omega\omega_y \\
&= \frac{4}{9\left(R_e^2 + R_i^2\right)}\left(\frac{R_e^3 - R_i^3}{R_e^2 - R_i^2}\right)^2 \pi^2 J\omega\omega_x + J\omega\omega_x \\
&\quad -\frac{4}{9\left(R_e^2 + R_i^2\right)}\left(\frac{R_e^3 - R_i^3}{R_e^2 - R_i^2}\right)^2 \pi^2 J\omega\omega_y \\
&\quad -\frac{8}{9\left(R_e^2 + R_i^2\right)}\left(\frac{R_e^3 - R_i^3}{R_e^2 - R_i^2}\right)^2 J\omega\omega_y,
\end{aligned}
\tag{32}
$$

where the signs (-) and (+) mean the clockwise and counterclockwise directions of the action of the inertial torques around two axes, respectively.

Simplification and transformation of Equation (32) yield the following:

$$
\omega_y = -\left[\frac{\left(8/\left(9\left(R_e^2 + R_i^2\right)\right)\right)\left(\left(R_e^3 - R_i^3\right)/\left(R_e^2 - R_i^2\right)\right)^2 \left(\pi^2 + 1\right) + 1}{1 - \left(8/\left(9\left(R_e^2 + R_i^2\right)\right)\right)\left(\left(R_e^3 - R_i^3\right)/\left(R_e^2 - R_i^2\right)\right)^2}\right]\omega_x.
\tag{33}
$$

The expressions of the inertial torques and their action, and the dependency of interrelated angular velocities of the spinning annulus around axes are presented in Table 2.

The expressions of torques and the dependency angular velocities (Table 2) formulate the mathematical models for the motions of the gyroscopic devices with the annulus rotor. Comparative analysis of formulas for the spinning annulus shows when its internal radius $R_i = 0$, all of them are converted to the formulas for the disc-type rotor presented in Table 1. This fact validates the mathematical correctness of the formulas. The values of formulas in Table 2 give results bigger than the formulas in Table 1.

5. Working Example

The annulus has a mass of 1.0 kg and the external and internal radii of 0.1 m and 0.06 m, respectively. The annulus rotates at

3000 rpm around the axle and precesses with an angular velocity of 0.06 rpm. Determine the values of the torques generated by the centrifugal and Coriolis force, the change in the angular momentum, and the angular velocity of precession. Substituting the data into equations of Table 2 and transformation yields the following results.

(i) The torque T_{ct} generated by the centrifugal forces

$$
\begin{aligned}
T_{ct} &= \frac{4}{9 \times \left(0.1^2 + 0.06^2\right)} \times \left(\frac{0.1^3 - 0.06^3}{0.1^2 - 0.06^2}\right)^2 \times \pi^2 \times 0.0068 \\
&\quad \times \frac{3000 \times 2\pi}{60} \times \frac{0.06 \times 2\pi}{60} = 0.06496634 Nm^2, \\
J &= \frac{1}{2} M\left(R_e^2 + R_i^2\right) = \frac{1}{2} \times 1.0 \times \left(0.1^2 + 0.06^2\right) = 0.0068 Nm^2.
\end{aligned}
\tag{34}
$$

(ii) The torque generated by Coriolis T_{cr} forces

$$
\begin{aligned}
T_{cr} &= \frac{8}{9 \times \left(0.1^2 + 0.06^2\right)} \times \left(\frac{0.1^3 - 0.06^3}{0.1^2 - 0.06^2}\right)^2 \times 0.0068 \\
&\quad \times \frac{3000 \times 2\pi}{60} \times \frac{0.06 \times 2\pi}{60} = 0.013164 Nm^2.
\end{aligned}
\tag{35}
$$

(iii) The torque T_{am} of the change in the angular momentum

$$
\begin{aligned}
T_{am} &= J\omega\omega_x = 0.0068 \times \frac{3000 \times 2\pi}{60} \times \frac{0.06 \times 2\pi}{60} \\
&= 0.013422 Nm^2.
\end{aligned}
\tag{36}
$$

(iv) The angular velocity of precession

$$
\begin{aligned}
\omega_y &= -\left[\frac{\left(8/\left(9 \times \left(0.1^2 + 0.06^2\right)\right)\right) \times \left(\left(0.1^3 - 0.06^3\right)/\left(0.1^2 - 0.06^2\right)\right)^2\left(\pi^2 + 1\right) + 1}{1 - \left(8/\left(9 \times \left(0.1^2 + 0.06^2\right)\right)\right) \times \left(\left(0.1^3 - 0.06^3\right)/\left(0.1^2 - 0.06^2\right)\right)^2}\right] \\
&\quad \times \frac{\left(0.06 \times 2\pi\right)}{60} = 3.816023 rad/s = 36.440337 rpm.
\end{aligned}
\tag{37}
$$

For the disc-type rotor (Table 1), the dependency of the angular velocities is obtained if the $R_i = 0$ in Table 2. Substituting data of the working example and computing yield:

$$
\omega_y = \left(8\pi^2 + 17\right) \times \frac{0.06 \times 2\pi}{60} = 0.602914 rad/s = 5.682336 rpm.
\tag{38}
$$

The comparative results of the dependency of the angular velocities rotation around axes of motions for the annulus and disc-type rotor show their big differences. The radius of disposition of the distributed mass of the annulus is bigger than for the disc-type rotor. Analysis of them yields the spinning annulus generates bigger values of the inertial torques and the dependency of the angular velocities than the spinning disc-type rotor.

6. Results and Discussion

Gyroscopic effects are remaining as sophisticated mathematical problems because the inertial torques generated by the rotating mass depend on the geometry of the spinning objects. The practice of engineering designs of the gyroscopic devices shows different geometry of their main components which are the rotors. The value of the inertial torques generated by the spinning rotors depends on their technical data. The working example shows the spinning annulus generates bigger values of the inertial torques and the dependency of the angular velocities than the disc-type rotor. This result gives the tip for the practitioners to design gyroscopic devices with a high value of the inertial torques and the angular velocity of precession. Practitioners can design gyroscopic devices with a necessary output of technical data that depends on the geometry of the spinning rotor. This result opens a new analytical approach to finding optimal designs of the spinning rotor that respond to the quality of gyroscope work.

7. Conclusion

Aerospace and engineering industries try to solve gyroscopic problems and find optimal designs for gyroscopic devices that give the necessary technical data. The new theory of gyroscopic effects for rotating objects opens new methods for computing the technical data for gyroscopic devices. The method for deriving mathematical models for the gyroscopic effects enables finding the output data of gyroscopic devices that depend on the geometry of the main unit which is the spinning rotor. Optimization of the rotor's design by criteria of the aerospace industry is a new direction for investigations in engineering. The fundamental principles of the theory of gyroscopic effects for rotating objects and methods enable solving them in engineering. The known numerical modeling for gyroscopic effects with expensive software is going past and engineering science receives new analytical methods.

Data Availability

The authors declare that the data supporting the findings of this study are available within the article. R. Usubamatov wrote the mathematical models of inertial torques. S. Kapayea corrected the text and references.

Conflicts of Interest

The authors declare that they have no conflicts of interest.

References

[1] F. J. B. Cordeiro, *The Gyroscope*, Createspace, NV, USA, 2015.

[2] G. Greenhill, *Report on Gyroscopic Theory*, Relink Books, Fallbrook, CA, USA, 2015.

[3] J. B. Scarborough, *The Gyroscope Theory and Applications*, Nabu Press, London, 2014.

[4] H. Weinberg, "Gyro mechanical performance: the most important parameter. Analog Devices," pp. 1–5, 2011, Technical Article MS2158.

[5] V. Apostolyuk, *Coriolis Vibratory Gyroscopes*, Springer International Publishing Switzerland, 2016.

[6] R. C. Hibbeler and K. B. Yap, *Mechanics for Engineers-Statics and Dynamics*, Prentice Hall, Pearson, Singapore, 14th ed. edition, 2020.

[7] D. R. Gregory, *Classical Mechanics*, Cambridge University Press, New York, 2012.

[8] J. R. Taylor, *Classical Mechanics*, University Science Books, California, USA, 2005.

[9] M. D. Aardema, *Analytical Dynamics*, Theory and Application, Academic/Plenum Publishers, New York, 2005.

[10] F. Scheck, *Mechanics*, Springer-Verlag, Berlin Heidelberg, 2018.

[11] M. M. Bhatti and E. E. Michaelides, "Oldroyd 6-constant electro-magneto-hydrodynamic fluid flow through parallel micro-plates with heat transfer using Darcy-Brinkman-Forchheimer model: a parametric investigation," *Mathematics in Engineering*, vol. 5, no. 3, pp. 1–19, 2022.

[12] W. C. Liang and S. C. Lee, "Vorticity, gyroscopic precession, and spin-curvature force," *Physical Review D*, vol. 87, no. 4, article 044024, 2013.

[13] J. L. Crassidis and F. L. Markley, "Three-axis attitude estimation using rate-integrating gyroscopes," *Journal of Guidance, Control, and Dynamics*, vol. 39, no. 7, pp. 1513–1526, 2016.

[14] Y. Nanamori and M. Takahashi, "An integrated steering law considering biased loads and singularity for control moment gyroscopes," in *AIAA Guidance, Navigation, and Control Conference*, Kissimmee, Florida, January 2015.

[15] Y. Chu and J. Fei, "Adaptive global sliding mode control for MEMS gyroscope using RBF neural network," *Mathematical Problems in Engineering*, vol. 2015, Article ID 403180, 9 pages, 2015.

[16] Q. Doukhi, A. R. Fayjie, and F. D. Jin Lee, "Intelligent controller design for quad-rotor stabilization in presence of parameter variations," *Journal of Advanced Transportation*, vol. 2017, Article ID 4683912, 10 pages, 2017.

[17] B. Xu and P. Zhang, "Minimal-learning-parameter technique based adaptive neural sliding mode control of MEMS gyroscope," *Complexity*, vol. 2017, Article ID 6019175, 8 pages, 2017.

[18] W. Wang, H. Ma, M. Xia, L. Weng, and X. Ye, "Attitude and altitude controller design for quad-rotor type MAVs," *Mathematical Problems in Engineering*, vol. 2013, Article ID 587098, 9 pages, 2013.

[19] Z. Zhu, Y. Bo, and C. Jiang, "A MEMS gyroscope noise suppressing method using neural architecture search neural network," *Mathematical Problems in Engineering*, vol. 2019, Article ID 5491243, 9 pages, 2019.

[20] R. Usubamatov, "Physics of gyroscope's "antigravity effect"," *Advances in Mathematical Physics*, vol. 2019, Article ID 4197863, 7 pages, 2019.

[21] R. Usubamatov and D. Allen, "Corrected inertial torques of gyroscopic effects," *Advances in mathematical physics*, vol. 2022, Article ID 3479736, 7 pages, 2022.

[22] R. Usubamatov, *Theory of Gyroscope Effects for Rotating Objects*, Springer, Cham, Switzerland, 2nd ed. edition, 2022.